

# Three-dimensional MR Cholangiopancreatography in a Breath Hold with Sparsity-based Reconstruction of Highly Undersampled Data<sup>1</sup>

Hersh Chandarana, MD  
Ankur M. Doshi, MD  
Alampady Shanbhogue, MD  
James S. Babb, PhD  
Mary T. Bruno, BS  
Tiejun Zhao, PhD  
Esther Raithe, PhD  
Michael O. Zenge, PhD  
Guobin Li, PhD  
Ricardo Otazo, PhD

## Purpose:

To develop a three-dimensional breath-hold (BH) magnetic resonance (MR) cholangiopancreatographic protocol with sampling perfection with application-optimized contrast using different flip-angle evolutions (SPACE) acquisition and sparsity-based iterative reconstruction (SPARSE) of prospectively sampled 5% k-space data and to compare the results with conventional respiratory-triggered (RT) acquisition.

## Materials and Methods:

This HIPAA-compliant prospective study was institutional review board approved. Twenty-nine patients underwent conventional RT SPACE and BH-accelerated SPACE acquisition with 5% k-space sampling at 3 T. Spatial resolution and other parameters were matched when possible. BH SPACE images were reconstructed by enforcing joint multicoil sparsity in the wavelet domain (SPARSE-SPACE). Two board-certified radiologists independently evaluated BH SPARSE-SPACE and RT SPACE images for image quality parameters in the pancreatic duct and common bile duct by using a five-point scale. The Wilcoxon signed-rank test was used to compare BH SPARSE-SPACE and RT SPACE images.

## Results:

Acquisition time for BH SPARSE-SPACE was 20 seconds, which was significantly ( $P < .001$ ) shorter than that for RT SPACE (mean  $\pm$  standard deviation, 338.8 sec  $\pm$  69.1). Overall image quality scores were higher for BH SPARSE-SPACE than for RT SPACE images for both readers for the proximal, middle, and distal pancreatic duct, but the difference was not statistically significant ( $P > .05$ ). For reader 1, distal common bile duct scores were significantly higher with BH SPARSE-SPACE acquisition ( $P = .036$ ). More patients had acceptable or better overall image quality (scores  $\geq 3$ ) with BH SPARSE-SPACE than with RT SPACE acquisition, respectively, for the proximal (23 of 29 [79%] vs 22 of 29 [76%]), middle (22 of 29 [76%] vs 18 of 29 [62%]), and distal (20 of 29 [69%] vs 13 of 29 [45%]) pancreatic duct and the proximal (25 of 28 [89%] vs 22 of 28 [79%]) and distal (25 of 28 [89%] vs 24 of 28 [86%]) common bile duct.

## Conclusion:

BH SPARSE-SPACE showed similar or superior image quality for the pancreatic and common duct compared with that of RT SPACE despite 17-fold shorter acquisition time.

©RSNA, 2016

<sup>1</sup>From the Center for Advanced Imaging Innovation and Research (CAI<sup>2</sup>R) (H.C., J.S.B., R.O.) and Bernard and Irene Schwartz Center for Biomedical Imaging (H.C., A.M.D., A.S., J.S.B., M.T.B., R.O.), Department of Radiology, New York University School of Medicine, 660 First Ave, New York, NY 10016; Siemens Healthcare, New York, NY (T.Z., M.O.Z.); Siemens Healthcare, Erlangen, Germany (E.R.); and Department of Radiology, Section of Medical Physics, Freiburg University Medical Center, Freiburg, Germany (G.L.). Received September 2, 2015; revision requested October 16; revision received November 3; accepted December 22; final version accepted January 5, 2016. The Center for Advanced Imaging Innovation and Research (CAI<sup>2</sup>R, [www.cai2r.net](http://www.cai2r.net)) at New York University School of Medicine is supported by NIH/NIBIB grant number P41 EB017183. Address correspondence to H.C. (e-mail: [hersh.chandarana@nyumc.org](mailto:hersh.chandarana@nyumc.org)).

**M**agnetic resonance (MR) cholangiopancreatography is an established noninvasive imaging method that is routinely used in clinical practice to assess biliary and pancreatic ductal anatomy to diagnose and study pancreatobiliary diseases (1–5). Current MR cholangiopancreatographic techniques are based on heavily T2-weighted fast spin-echo pulse sequences and have evolved from a two-dimensional thick-slab acquisition to a three-dimensional (3D) near-isotropic volumetric acquisition (6–8). Because 3D isotropic or near-isotropic acquisition with volumetric coverage cannot be performed routinely in a breath hold (BH) because of the large amount of k-space data required, it is routinely performed with a prospective respiratory-triggered (RT) technique (9,10). Although prospective RT enables isotropic 3D volumetric MR cholangiopancreatography, it is inefficient, because data acquisition is performed only during a short portion of the respiratory cycle. Furthermore, in patients with shallow or irregular respiratory rhythm, respiratory-gated acquisitions may fail to trigger correctly, which can further prolong the imaging times and can result in image quality degradation such as blurring (11).

### Advances in Knowledge

- Diagnostic three-dimensional MR cholangiopancreatography can be performed during breath hold and images can be reconstructed with sparsity-based iterative reconstruction (SPARSE) from prospectively sampled 5% k-space data.
- Image quality parameter scores for the pancreatic duct and the common bile duct were similar or higher with breath-hold SPARSE from prospectively sampled 5% k-space data when compared with conventional respiratory-triggered navigated MR cholangiopancreatography, with a lower failure rate despite approximately 17-fold acceleration.

Sampling perfection with application-optimized contrast using different flip angle evolutions (SPACE) is a 3D fast spin-echo acquisition technique (12) that allows for high-spatial-resolution volumetric MR cholangiopancreatography with excellent image quality and has been shown to be superior at 3 T when compared with 1.5-T field strength (8,13). However, prospectively RT SPACE MR cholangiopancreatography routinely requires 3–6 minutes of acquisition time (8) and may result in suboptimal image quality in patients who do not have a consistent breathing pattern.

Sparsity-based reconstruction techniques have been used to accelerate data acquisition by enabling accurate reconstructions from undersampled k-space data if (a) underlying images are sparse or compressible either in image domain or in some transform domain and (b) the undersampling scheme is incoherent (14–19). The first condition implies that the number of pixels with information is much lower than the total number of pixels in that domain, and the second condition requires that artifacts due to k-space undersampling be different from image features. MR cholangiopancreatographic images are acquired with strong T2 weighting, which suppresses most of the anatomic background. The diagnostic information is contained mostly in the small number of voxels in the pancreatic and biliary ducts that have sufficiently high T2 value. Since the ducts occupy a small region in the field of view, the resulting MR cholangiopancreatographic image is sparse. Given this sparsity, it may be possible to acquire only a small portion of the k-space data prospectively during BH and reconstruct images with a sparsity-based iterative reconstruction (SPARSE) of prospectively sampled 5%

### Implication for Patient Care

- Three-dimensional breath-hold MR cholangiopancreatography may be a substitute for conventional respiratory-triggered MR cholangiopancreatography or may serve as an add-on sequence to decrease the failure rate of MR cholangiopancreatography.

k-space. SPARSE with sensitivity encoding is one such approach that combines sparsity and parallel imaging in a joint reconstruction algorithm that enables higher acceleration rates (18) than any technique alone. Therefore, the aim of this study was to develop 3D MR cholangiopancreatography by using BH SPARSE-SPACE and to compare it with conventional RT SPACE imaging in patients undergoing a clinically indicated examination.



### Materials and Methods

Three of the authors are employees of Siemens Healthcare. These authors provided technical assistance but were not involved in the data acquisition and evaluation, and they did not have direct control of the data.

### Patients

This Health Insurance Portability and Accountability Act-compliant prospective study was performed after institutional review board approval was obtained. A total of 375 patients

### Published online before print

10.1148/radiol.2016151935 **Content codes:**  

**Radiology 2016;** 280:585–594

### Abbreviations:

BH = breath hold

RT = respiratory triggered

SPACE = sampling perfection with application optimized contrast using different flip angle evolutions

SPARSE = sparsity-based iterative reconstruction

3D = three-dimensional

### Author contributions:

Guarantor of integrity of entire study, H.C.; study concepts/study design or data acquisition or data analysis/interpretation, all authors; manuscript drafting or manuscript revision for important intellectual content, all authors; approval of final version of submitted manuscript, all authors; agrees to ensure any questions related to the work are appropriately resolved, all authors; literature research, H.C., E.R., R.O.; clinical studies, H.C., A.M.D., A.S., M.T.B.; experimental studies, M.T.B., T.Z., M.O.Z., G.L., R.O.; statistical analysis, H.C., J.S.B.; and manuscript editing, H.C., A.M.D., J.S.B., M.T.B., T.Z., E.R., R.O.

### Funding:

This research was supported by the National Institutes of Health (grant P41 EB017183).

Conflicts of interest are listed at the end of this article.

underwent clinically indicated MR cholangiopancreatography at the outpatient facility of our institution from October 1, 2014 to April 1, 2015. Of these, 312 patients were imaged with an MR imager that did not have the prototype sequence available and thus were excluded. The remaining 63 patients were imaged with the 3-T MR imaging system (Magnetom Skyra; Siemens Healthcare, Erlangen, Germany) that included the prototype BH accelerated SPACE research sequence. Of these 63 patients, 32 did not agree to participate in the study and were excluded. Thus, 31 patients agreed to participate in the study and provided written informed consent. One patient was excluded because the raw data for the off-line BH SPARSE-SPACE reconstruction was not saved, and one patient was unable to complete the conventional RT SPACE sequence because of claustrophobia and was excluded. Thus, 29 patients, 19 women (mean age, 62 years; range, 34–88 years) and 10 men (mean age, 58 years; range, 37–86 years), underwent both BH SPARSE-SPACE and RT SPACE MR cholangiopancreatography and constituted our study cohort.

Patients were referred for MR cholangiopancreatography for the following clinical indications: (a) diagnosis or follow-up of a pancreatic cyst or cystic lesion ( $n = 9$ ), (b) known or suspected pancreatic mass or malignancy ( $n = 7$ ), (c) abnormal blood test (liver function or lipase) ( $n = 5$ ), (d) abdominal pain ( $n = 3$ ), (e) primary biliary cirrhosis ( $n = 2$ ), (f) primary sclerosing cholangitis ( $n = 1$ ), and (g) follow-up after liver transplantation ( $n = 2$ ).

### MR Imaging

Imaging was performed with a 3-T system (Magnetom Skyra, Siemens Healthcare) on which the prototype BH MR cholangiopancreatographic accelerated SPACE sequence was available. An 18-channel body-array coil and an eight-channel posterior spine coil were used for MR imaging. Patients were randomized to undergo conventional RT SPACE before BH SPARSE-SPACE for examinations performed on odd number dates or BH SPARSE with

sensitivity encoding before RT SPACE on even number dates.

**Conventional RT acquisition.**—The RT SPACE acquisition is a component of our routine clinical MR cholangiopancreatographic protocol and was performed with the following acquisition parameters: repetition time, variable depending on the respiratory rate; echo time, 812 msec; flip angle, 100°; parallel imaging acceleration factor, three; spectrally selective fat saturation to suppress signal intensity from fat; base resolution, 384; section thickness, 1.1 mm; resolution (interpolated),  $1 \times 1 \times 1.1$  mm; number of coronal sections, 90; and acquisition time, variable.

**BH SPARSE-SPACE acquisition.**—An accelerated SPACE pulse sequence prototype was developed by using a variable-density Poisson-disk random undersampling pattern of the two phase-encoding dimensions (20). This sampling pattern is suitable for the combination of sparsity and parallel imaging as used in SPARSE with sensitivity encoding, because it contains sufficient incoherence and avoids gaps in k-space that can result from use of a conventional random distribution. A technique for trajectory optimization was used to prevent strong echo-train fluctuations in the highly undersampled data. Five percent of k-space data was acquired on a coronal plane during a 20-second BH with the following acquisition parameters: repetition time msec/echo time msec, 2000/812; flip angle, 100°; spectrally selective fat saturation to saturate fat signal intensity; parallel imaging acceleration factor, two; base resolution, 384; section thickness, 1.1 mm; and resolution (interpolated),  $1 \times 1 \times 1.1$  mm. A total of 64 sections in coronal plane with 100% section oversampling were acquired to match the acquisition volume of conventional RT SPACE.

**BH SPARSE-SPACE reconstruction.**—Image reconstruction was performed by enforcing joint multicoil sparsity in the wavelet space of the 3D MR cholangiopancreatographic images on the basis of the SPARSE with sensitivity encoding method (18). The wavelet transformation is a common compression transform used in

the JPEG2000 standard (Joint Photographic Experts Group) that produces sparser representations of the MR cholangiopancreatography by exploiting spatial correlations between edges (21). SPARSE with sensitivity-encoding reconstruction was implemented by using a fast iterative soft-thresholding algorithm (22) with a redundant 3D Haar wavelet transform to solve sparsity-based optimization problems with comparatively fast convergence and low computational burden. The algorithm uses soft thresholding in the wavelet space of the image, resulting from the contribution from all coils to enforce sparsity (by keeping the high-value coefficients and excluding the low-value coefficients) followed by coil-by-coil evaluation of data consistency to ensure that the reconstructed image is compatible with the acquired data (Fig 1) (23). This algorithm was implemented in the C++ programming language by using multithread programming and was integrated on a standard clinical imaging reconstruction computer.

### Image Analysis

BH SPARSE-SPACE MR cholangiopancreatographic data (in Digital Imaging and Communications in Medicine format) and conventional RT SPACE data were anonymized and presented in random order to two board-certified radiologists (A.S. and A.M.D., with approximately 5 and 2 years of clinical experience in interpretation of MR examinations, respectively) who performed image analysis independently. Readers were aware of the clinical indication but no other clinical information was provided. No data from pulse sequences other than anonymized MR cholangiopancreatography were made available to the readers. The readers underwent a short training session before image evaluation. The readers evaluated overall image quality, clarity, and sharpness of the proximal, middle, and distal pancreatic duct; proximal and distal common bile duct; and cystic duct by using a five-point scale (1–5), with higher scores indicating better image quality (Table 1). Presence or absence of pancreatic lesions was noted by the readers. Lesion

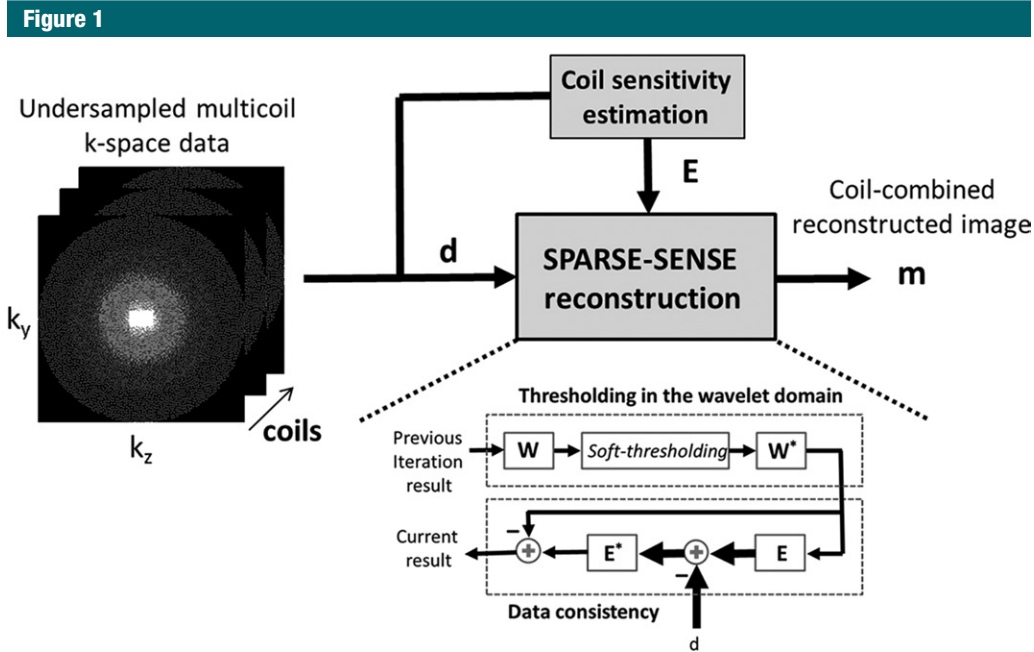


**Figure 1:** Illustration shows data acquisition and image reconstruction for SPARSE-SPACE method. Three-dimensional k-space data ( $d$ ) are acquired by using Poisson-disk random undersampling pattern, which presents favorable conditions for SPARSE with sensitivity encoding (*SENSE*) approach. Fully sampled center is used to calculate coil sensitivity and the data acquisition operator ( $E$ ). SPARSE with sensitivity-encoding reconstruction algorithm iteratively enforces sparsity in wavelet domain ( $W$ ) by thresholding low-value coefficients and checking data consistency in k-space for each coil. After number of iterations (usually 20–25), the reconstruction algorithm will find the sparsest solution that is consistent with the acquired data, resulting in a unaliased image.  $m$  = reconstructed image,  $*$  = backward operator.

conspicuity and lesion edge sharpness also were evaluated by using a five-point scale (Table 1). Acquisition time for the BH examination was 20 seconds in all subjects. The acquisition time for the RT SPACE acquisition was variable, depending on respiratory rate and triggering efficiency. Data were captured from the Digital Imaging and Communications in Medicine header for each subject and were tabulated.

**Statistical Analysis**

A paired-sample  $t$  test was used to compare acquisition time between the BH SPARSE-SPACE and RT SPACE images for each subject. The image-quality scores for each quality metric (overall image quality, duct clarity, and duct sharpness) for each morphologic duct segment (proximal, middle, and distal pancreatic duct; proximal and distal common bile duct; and cystic duct) was tabulated for both readers for BH SPARSE-SPACE and RT SPACE.

**Table 1**

Image Quality Parameter Scores		
Image Quality Parameter	Score	Scoring System
Overall image quality	1–5	1, nondiagnostic; 2, poor; 3, acceptable; 4, good; 5, excellent
Duct sharpness	1–5	1, nondiagnostic; 2, extreme blur; 3, moderate blur; 4, mild blur; 5, no blur
Duct visualization	1–5	1, not visualized; 2, poorly visualized; 3, partially visualized; 4, well visualized; 5, Excellently visualized
Lesion conspicuity	1–5	1, unreadable; 2, poor; 3, acceptable; 4, good; 5, excellent
Lesion edge sharpness	1–5	1, unreadable; 2, extreme blur; 3, moderate blur; 4, mild blur; 5, no blur

Mean, standard deviation, and range for each measure of image quality for each ductal segment as determined by each reader were computed.

The within-subject difference between the conventional and BH acquisitions in image quality scores at each site as determined by each reader was computed as the score for BH SPARSE-SPACE minus the score for RT SPACE. Exact Wilcoxon signed-rank tests were applied to the within-subject differences to compare the acquisitions for image

quality. The linearly weighted  $\kappa$  coefficients were computed to assess reader agreement on overall image quality. The  $\kappa$  value is typically interpreted as an indication of poor agreement when it is less than zero, as slight agreement when  $\kappa$  is 0–0.2, as fair agreement when  $\kappa$  is 0.2–0.4, as moderate agreement when  $\kappa$  is 0.4–0.6, substantial agreement when  $\kappa$  is 0.6–0.8, and perfect agreement when  $\kappa$  is 0.8–1.0 (24).

The number and percentage of times the overall image quality score



Table 2

## Image Quality Scores for the Pancreatic Duct

Pancreatic Duct Segment and Reader	Overall Image Quality		Duct Visualization		Duct Sharpness	
	BH SPARSE	RT SPACE	BH SPARSE	RT SPACE	BH SPARSE	RT SPACE
<b>Proximal</b>						
Reader 1	3.69 ± 1.4 (1–5)	3.38 ± 1.4 (1–5)	3.83 ± 1.3 (1–5)	3.45 ± 1.2 (1–5)	3.72 ± 1.4 (1–5)	3.41 ± 1.3 (1–5)
Reader 2	3.83 ± 1.0 (2–5)	3.69 ± 1.3 (1–5)	4.1 ± 1.0 (2–5)	4.1 ± 1.0 (1–5)	3.72 ± 0.9 (2–5)	3.41 ± 1.1 (1–5)
<b>Middle</b>						
Reader 1	3.59 ± 1.4 (1–5)	3.14 ± 1.4 (1–5)	3.69 ± 1.4 (1–5)*	3.21 ± 1.3 (1–5)*	3.62 ± 1.4 (1–5)	3.14 ± 1.4 (1–5)
Reader 2	3.62 ± 1.1 (1–5)	3.55 ± 1.2 (1–5)	3.97 ± 1.0 (1–5)	3.93 ± 1.2 (1–5)	3.62 ± 1.1 (1–5)	3.48 ± 1.2 (1–5)
<b>Distal</b>						
Reader 1	3.31 ± 1.3 (1–5)	2.83 ± 1.4 (1–5)	3.38 ± 1.3 (1–5)*	2.86 ± 1.3 (1–5)*	3.38 ± 1.3 (1–5)	2.86 ± 1.4 (1–5)
Reader 2	3.14 ± 1.0 (1–5)	2.72 ± 1.1 (1–5)	3.38 ± 1.0 (1–5)	3.0 ± 1.0 (1–5)	3.0 ± 1.0 (1–5)	2.62 ± 1.0 (1–5)

Note.—Data are means standard deviation, with range of scores in parentheses. Scores for all image quality parameters were similar or higher with BH SPARSE than with RT SPACE.

\* Difference between BH SPARSE and RT SPACE scores was significant for pancreatic duct ( $P = .049$ ) and distal pancreatic duct ( $P = .038$ ) for reader 1.

was greater than or equal to 3 (acceptable or better) for one acquisition but less than 3 (less than acceptable) for the other acquisition also were computed for each duct segment, and reader scores were averaged. Similarly, mean and standard deviation of each image quality parameter for the pancreatic lesions were computed from the scores provided by each reader for each lesion for both sequences. A paired-sample Wilcoxon signed-rank test was used to compare sequences for pancreatic lesion conspicuity and lesion edge sharpness. All statistical tests were conducted with a two-sided test and 5% significance level by using SAS 9.3 (SAS Institute, Cary, NC).

## Results

### Acquisition Time

Acquisition time for BH SPARSE-SPACE was 20 seconds in each subject. This was significantly shorter than the acquisition time for RT SPACE ( $P < .001$ ), which was 338.8 seconds ± 69.1 (range, 193–479 seconds). Thus, BH SPARSE-SPACE was approximately 17-fold faster than RT SPACE.

### Pancreatic Duct

Overall image quality scores were higher for BH SPARSE-SPACE than for RT SPACE in the proximal, middle, and

distal pancreatic duct for both readers (Tables 2, 3), but this difference was not statistically significant for either reader (all  $P > .05$ ). Duct sharpness scores were not significantly different between BH SPARSE-SPACE and RT SPACE for both readers (all  $P > .05$ ), although there was a tendency for higher scores with BH SPARSE. Scores for duct visualization were higher with BH SPARSE-SPACE than with RT SPACE for reader 1 for the proximal, middle, and distal pancreatic duct, and this difference was statistically significant for the middle ( $3.69 ± 1.4$  vs  $3.21 ± 1.3$ , respectively;  $P = .049$ ) and distal ( $3.38 ± 1.3$  vs  $2.86 ± 1.3$ , respectively;  $P = .038$ ) pancreatic duct (Fig 2). Scores for duct visualization were similar for BH SPARSE-SPACE and RT SPACE for reader 2 without a significant difference (all  $P > .05$ ). More patients had acceptable or better overall image quality (scores greater or equal to 3) with BH SPARSE-SPACE than with RT SPACE, respectively, for the proximal (23 of 29 [79%] vs 22 of 29 [76%]), middle (22 of 29 [76%] vs 18 of 29 [62%]), and distal (20 of 29 [69%] vs 13 of 29 [45%]) pancreatic duct.

### Common Bile Duct and Cystic Duct

Overall image quality scores for the proximal and distal common bile duct and cystic duct were higher with BH SPARSE-SPACE compared with RT

SPACE for reader 1, and these differences were statistically significant for the distal common bile duct ( $4.14 ± 1.1$  vs  $3.79 ± 1.1$ ;  $P = .036$ ) and cystic duct ( $3.46 ± 1.4$  vs  $2.81 ± 1.3$ ;  $P = .037$ ) (Fig 3). For reader 2, the scores with BH SPARSE-SPACE were not significantly different compared with RT SPACE for the proximal and distal common bile duct and cystic duct (all  $P > .05$ ) (Tables 4, 5). Scores for duct sharpness were similar between BH SPARSE-SPACE and RT SPACE for proximal and distal common bile duct for both readers, as well as for cystic duct for reader 2 without statistically significant differences (all  $P > .05$ ). For reader 1, the score for cystic duct sharpness was significantly higher with BH SPARSE-SPACE compared with RT SPACE ( $3.46 ± 1.4$  versus  $2.81 ± 1.3$ , respectively;  $P = .037$ ). Duct visualization scores were higher with BH SPARSE-SPACE for proximal and middle common bile duct and cystic duct for reader 1, and this was statistically significant for distal common bile duct ( $4.43 ± 0.9$  vs  $3.82 ± 1.2$ , respectively;  $P = .011$ ) and cystic duct ( $3.54 ± 1.3$  vs  $2.88 ± 1.3$ , respectively;  $P = .037$ ). For reader 2, these scores were similar between BH SPARSE-SPACE and RT SPACE without significant differences (all,  $P > .05$ ). More patients had acceptable or better overall image quality (scores equal or greater than 3)

with BH SPARSE-SPACE than with RT SPACE for proximal (25 of 28 [89%] vs 22 of 28 [79%], respectively) and distal (25 of 28 [89%] vs of 24 of 28 [86%], respectively) common bile duct.

### Interreader Agreement

Moderate to substantial agreement was noted between the two readers ( $\kappa = 0.42$  and  $0.67$  for readers 1 and 2,

respectively) for the overall image quality scores of the pancreatic, cystic, and common ducts (Table 6).

### Pancreatic Lesions

A total of 13 pancreatic lesions were detected by reader 1 in 13 subjects on images from both sequences. For reader 1, there were no statistically significant differences (all,  $P > .05$ )

between BH SPARSE-SPACE and RT SPACE in scores for lesion conspicuity ( $4.9 \pm 0.2$  vs  $4.85 \pm 0.4$ , respectively) or lesion edge sharpness ( $3.92 \pm 0.6$  vs  $3.92 \pm 0.9$ , respectively) (Fig 4). Reader 2 identified 12 pancreatic lesions in 12 patients on images from both sequences. For reader 2, there were no statistically significant differences (all  $P > .05$ ) between BH SPARSE-SPACE and RT SPACE in scores for lesion conspicuity ( $4.42 \pm 0.8$  vs  $4.17 \pm 0.7$ , respectively) or lesion edge sharpness ( $4.08 \pm 0.8$  vs  $4.0 \pm 0.7$ , respectively).

**Table 3**

### Difference in Image Quality Scores between Techniques in Pancreatic Duct

Image Quality Score Combination	Part of Pancreatic Duct ( $n = 29$ )		
	Proximal	Middle	Distal
Acceptable BH SPARSE-SPACE and unacceptable RT SPACE score	4 (14)	7 (24)	9 (31)
Acceptable RT SPACE and unacceptable BH SPARSE-SPACE score	3 (10)	3 (10)	2 (7)

Note. Data are number of subjects, with percentage in parentheses. Acceptable scores were those greater than or equal to 3, unacceptable scores were those less than 3.

### Discussion

Single BH 3D MR cholangiopancreatography is feasible with 5% k-space sampling and SPARSE with sensitivity-encoding reconstruction. BH

**Figure 2**

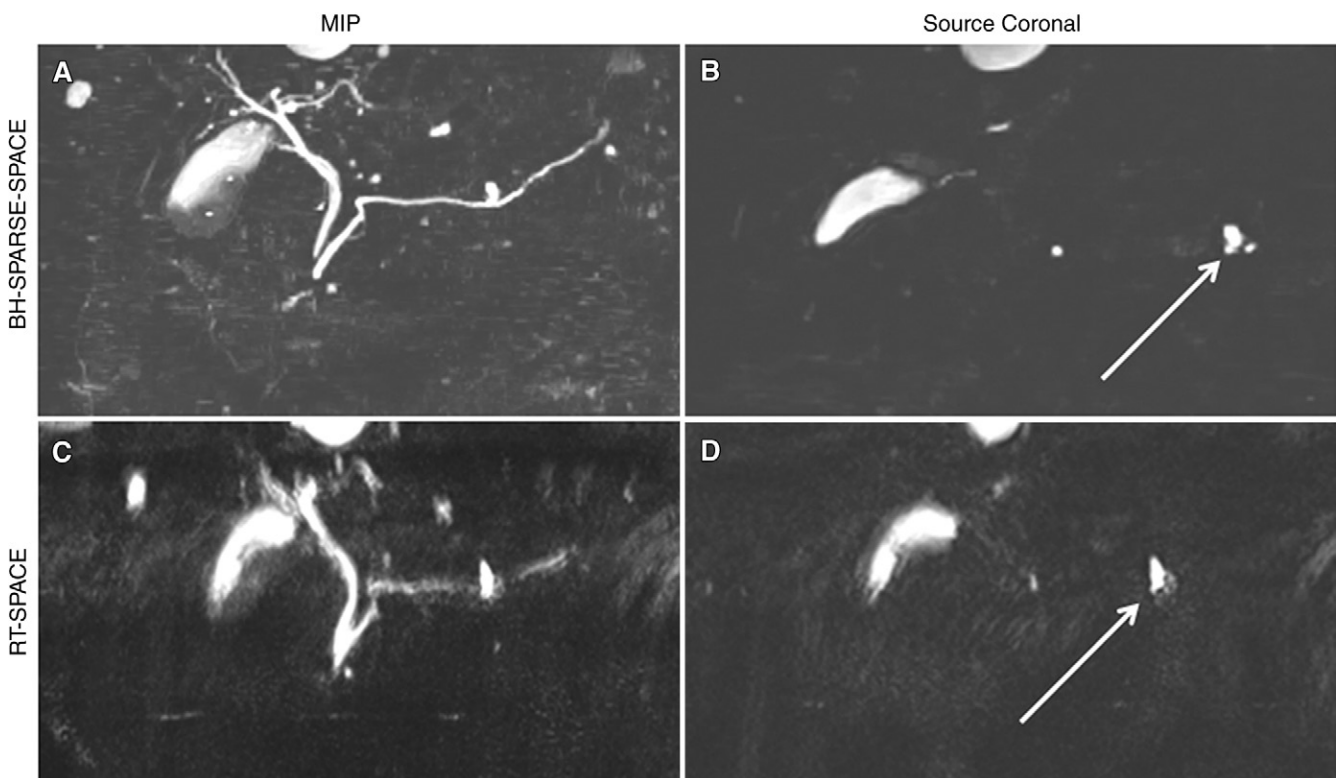


**Figure 2:** BH SPARSE-SPACE and conventional RT SPACE MR cholangiopancreatographic images in a 64-year-old woman suspected of having pancreatic lesion. A, BH SPARSE-SPACE maximum intensity projection (MIP) image and, B, source image in coronal plane demonstrate image quality equal to or better than that of, C, conventional RT SPACE maximum intensity projection and, D, source image for pancreatic duct. Ductal communication of pancreatic cystic lesion was better shown with BH SPARSE-SPACE (arrow, B) than with RT SPACE (arrow, D).

**Figure 3**

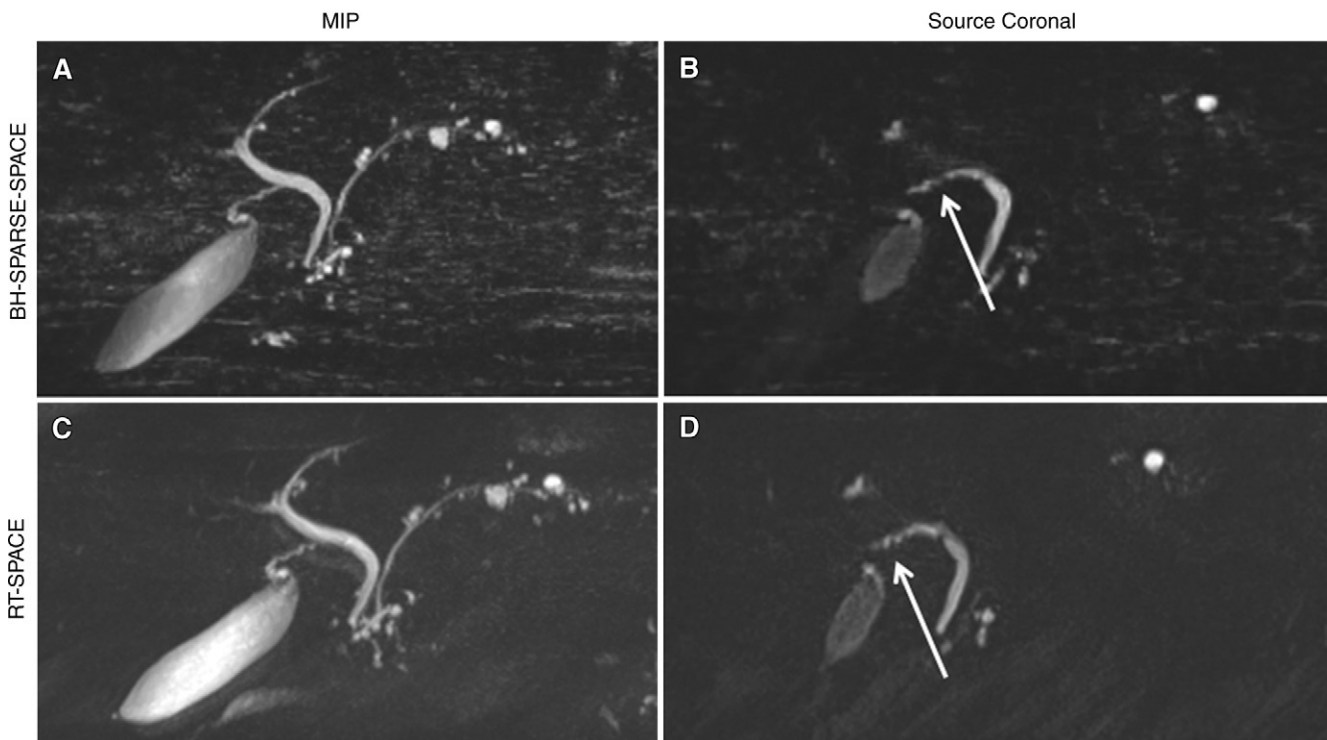


**Figure 3:** BH SPARSE-SPACE MR cholangiopancreatography and conventional RT SPACE MR cholangiopancreatographic images in a 68-year-old woman with history of pancreatic cysts. *A*, Maximum intensity projection (*MIP*) and, *B*, source image on coronal plane show image quality equal to or better than that of, *C*, conventional RT SPACE maximum intensity projection and, *D*, source images for common duct and cystic duct. Cystic duct (arrow) was equally well visualized with BH SPARSE-SPACE and RT SPACE.

**Table 4**

**Image Quality Scores for Common Bile Duct and Cystic Duct**

Bile Duct Segment and Reader	Overall Image Quality*		Duct Visualization†		Duct Sharpness‡	
	BH SPARSE	RT SPACE	BH SPARSE	RT SPACE	BH SPARSE	RT SPACE
<b>Proximal common bile duct (n = 28)<sup>§</sup></b>						
Reader 1	4.21 ± 1.2 (1–5)	3.71 ± 1.2 (2–5)	4.36 ± 1.0 (1–5)	3.86 ± 1.1 (2–5)	4.11 ± 1.1 (1–5)	3.75 ± 1.1 (2–5)
Reader 2	4.07 ± 0.9 (2–5)	4.07 ± 1.0 (2–5)	4.5 ± 0.8 (2–5)	4.46 ± 0.7 (3–5)	3.79 ± 0.8 (2–5)	4.0 ± 1.0 (2–5)
<b>Distal common bile duct (n = 28)</b>						
Reader 1	4.14 ± 1.1 (1–5)	3.79 ± 1.1 (2–5)	4.43 ± 0.9 (1–5)	3.82 ± 1.2 (2–5)	4.14 ± 1.1 (1–5)	3.79 ± 1.1 (2–5)
Reader 2	4.11 ± 0.9 (2–5)	4.07 ± 0.9 (2–5)	4.54 ± 0.7 (2–5)	4.43 ± 0.6 (3–5)	4.11 ± 0.9 (2–5)	4.07 ± 0.9 (2–5)
<b>Cystic duct (n = 26)<sup>  </sup></b>						
Reader 1	3.46 ± 1.4 (1–5)	2.81 ± 1.3 (1–5)	3.54 ± 1.3 (1–5)	2.88 ± 1.3 (1–5)	3.46 ± 1.4 (1–5)	2.81 ± 1.3 (1–5)
Reader 2	3.36 ± 1.2 (1–5)	3.28 ± 1.3 (1–5)	3.52 ± 1.3 (1–5)	3.44 ± 1.2 (1–5)	3.24 ± 1.1 (1–5)	3.12 ± 1.1 (1–5)

Note.—Data are means ± standard deviation, with range of scores in parentheses.

\* For reader 1, BH SPARSE scores were significantly higher than RT SPACE scores for distal common bile duct ( $P = .036$ ) and cystic duct ( $P = .037$ ).

† For reader 1, duct visualization scores were significantly higher for BH SPARSE than for RT SPACE for distal common bile duct ( $P = .011$ ) and cystic duct ( $P = .037$ ).

‡ For reader 1, sharpness of cystic duct scores were significantly higher for BH SPARSE-SPACE than for RT SPACE ( $P = .037$ ).

§ One patient with prior liver transplant had choledochojejunostomy, and hence, common bile duct was not assessed.

|| Three patients had absence of cystic duct due to prior surgeries, and hence, cystic duct was not assessed

Table 5

**Difference in Image Quality Scores between Techniques in Common Bile and Cystic Ducts**

Image Quality Score Combination	Common Bile Duct (n = 28)		Cystic Duct (n = 26)
	Proximal	Middle	
Acceptable BH SPARSE-SPACE and unacceptable RT SPACE score	5 (18)	3 (11)	6 (23)
Acceptable RT SPACE and unacceptable BH SPARSE-SPACE score	2 (7)	2 (7)	2 (8)

Note.—Data are number of patients, with percentage in parentheses. Acceptable scores were those greater than or equal to 3, unacceptable scores were those less than 3.

SPARSE-SPACE MR cholangiopancreatography demonstrates image quality that is equal or superior to that of conventional RT SPACE MR cholangiopancreatography for the pancreatic duct and the common bile duct. These results are encouraging, because despite nearly 17-fold acceleration, diagnostic image quality was maintained with the BH SPARSE-SPACE technique with a lower failure rate than that with the conventional RT SPACE method. The ability to reconstruct images faithfully from only 5% of the k-space suggests that MR cholangiopancreatographic images are very compressible in the wavelet domain, and the use of the appropriate sparsity-based reconstruction approach allowed for high acceleration in this study.

Conventional image quality metrics such as signal-to-noise ratio or contrast-to-noise ratio are challenging to compute and interpret due to the nonlinearity of iterative image reconstruction, and hence, were not used in this study. Such metrics, moreover, do not capture the principal failure modes of sparsity-based reconstructions, such as suppression of low-contrast features and blurring and synthetic-appearing image structure (25). Qualitative impressions from board-certified abdominal radiologists were thus used in this study to evaluate image quality.

The noise pattern and image texture of the BH SPARSE-SPACE reconstruction, as expected, were slightly different when compared with those of the conventional RT SPACE acquisition. Despite these differences, both readers

scored the image quality of the BH SPARSE images to be equal to or better than that of the conventional RT SPACE images. It seems that the readers were able to tolerate the differences in noise and texture pattern, and this did not affect their ability to assess image quality. In this study, there were no statistically significant differences between BH SPARSE-SPACE and RT SPACE images in pancreatic lesion conspicuity and sharpness. However, a larger study will be required to test the accuracy and sensitivity of BH SPARSE-SPACE MR cholangiopancreatography for detection and characterization of pancreatic and biliary lesions. Furthermore, because of the differences in noise pattern and image texture, the readers may have been unblinded inadvertently, which was a limitation of the study.

SPARSE reconstruction with sensitivity encoding has been used primarily for dynamic imaging (16,26), because dynamic images are more compressible than are static images. This work represents an application of SPARSE with sensitivity encoding to static imaging, which was possible due to the high sparsity of the MR cholangiopancreatographic images. We also have replaced the original conjugate-gradient optimization in SPARSE with sensitivity encoding with the fast iterative soft-thresholding algorithm, a much faster and less-demanding algorithm that can shorten reconstruction times in a clinical system.

Several other approaches have been proposed to accelerate MR cholangiopancreatographic acquisition. Such approaches involve use of a single-shot

Table 6

**Interreader Agreement for Overall Image Quality for BH SPARSE-SPACE and RT SPACE Acquisitions**

Ductal Segment	BH SPARSE-SPACE	RT SPACE
Proximal pancreatic duct	0.57	0.59
Middle pancreatic duct	0.62	0.59
Distal pancreatic duct	0.59	0.44
Proximal common bile duct	0.52	0.53
Distal common bile duct	0.59	0.44
Cystic duct	0.67	0.51

Note.—Data are  $\kappa$  coefficients.

fast spin-echo or balanced steady-state free-precession sequence to achieve acceleration (27,28). However, these techniques sacrifice volumetric coverage or near-isotropic spatial resolution, or change the image contrast. Our proposed approach uses a SPACE sequence that is modified to permit undersampling while maintaining the T2 contrast. Direct comparison of these various acceleration methods for detection and characterization of pancreatobiliary abnormality with conventional navigated acquisition serving as a reference would be of interest. However, many of these techniques are not yet commercially available for direct comparison.

There were several limitations to our study. First, we used only 5% of the k-space for the reconstructions. A detailed optimization of k-space sampling versus image quality and acquisition time was not performed because of our desire to acquire all the necessary data in a single BH. A triggered SPARSE-SPACE approach is under investigation, where we can tailor and assess the effect of k-space acquisition on image quality and time while not relying on the BH capacity of the patient. Second, only a small number of patients were included in our study. A larger study will be required to compare BH SPARSE-SPACE and RT SPACE for lesion detection and characterization. Outpatients were included in our study because



Figure 4

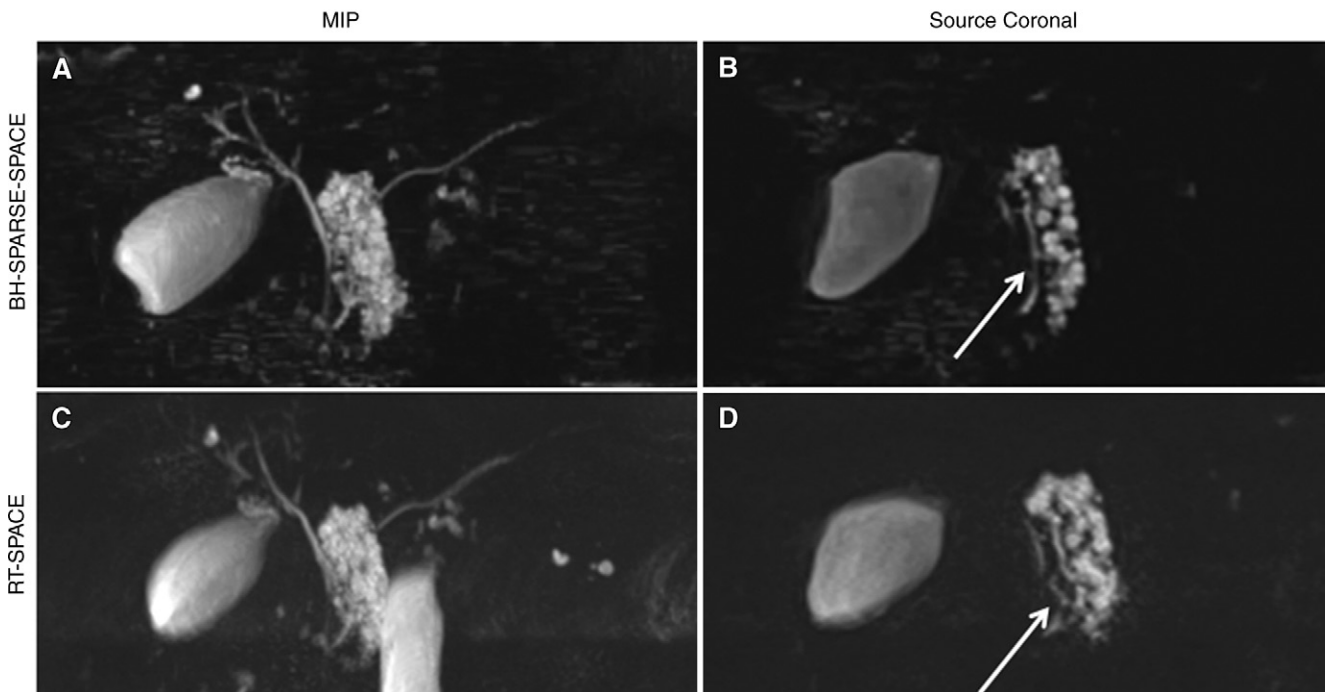


**Figure 4:** BH SPARSE-SPACE MR cholangiopancreatographic and conventional RT SPACE images in a 58-year-old woman with known pancreatic cystic lesion. BH SPARSE-SPACE, *A*, maximum intensity projection (*MIP*) and, *B*, source image on coronal plane better show communication of cystic lesion with pancreatic duct when compared with, *C*, conventional RT SPACE maximum intensity projection and, *D*, source image. Demonstration of this ductal communication helped the radiologist with diagnosis of side-branch intraductal papillary mucinous neoplasm (arrow).

the prototype sequence was available on the MR system located in the outpatient facility. Hospitalized or sick patients may not be able to suspend respiration for 20 seconds. The effect of inadequate BH on image quality was not evaluated. It is possible that some of our patients were not able to tolerate a 20-second BH and this could have resulted in compromised image quality with our technique. However, in this study, we did not exclude any patients on the basis of BH capacity. In the future, patients may be stratified to undergo BH MR cholangiopancreatography if they have good BH capacity or may undergo a navigated scheme if they have poor BH capacity. This will be the focus of our investigation in the near future. Interobserver agreement between the readers for subjective evaluation of image quality was moderate to substantial despite readers undergoing a training session before image assessment.

In conclusion, in our study we showed that it is possible to use SPARSE-SPACE to acquire diagnostic-quality MR cholangiopancreatographic images during a 20-second BH. The image quality as assessed by the two readers was comparable to or better than that with the conventional navigated acquisition method and with a lower failure rate despite more than 17-fold acceleration. The proposed approach of BH SPARSE-SPACE has the potential to improve MR cholangiopancreatography either as an add-on to the conventional MR cholangiopancreatographic protocol to improve robustness or as a replacement for RT acquisition in subjects with good BH capacity.

**Disclosures of Conflicts of Interest:** **H.C.** Activities related to the present article: non-financial support from Siemens Health Care. Activities not related to the present article: member of advisory board for Siemens, grant from RSNA. Other relationships: disclosed no relevant relationships. **A.M.D.** disclosed no relevant relationships. **A.S.** disclosed no relevant

relationships. **J.S.B.** disclosed no relevant relationships. **M.T.B.** disclosed no relevant relationships. **T.Z.** Activities related to the present article: disclosed no relevant relationships. Activities not related to the present article: employment with Siemens. Other relationships: disclosed no relevant relationships. **E.R.** disclosed no relevant relationships. **M.O.Z.** Activities related to the present article: employment with Siemens. Activities not related to the present article: disclosed no relevant relationships. Other relationships: disclosed no relevant relationships. **G.L.** disclosed no relevant relationships. **R.O.** disclosed no relevant relationships.

## References

1. Kaltenthaler E, Vergel YB, Chilcott J, et al. A systematic review and economic evaluation of magnetic resonance cholangiopancreatography compared with diagnostic endoscopic retrograde cholangiopancreatography. *Health Technol Assess* 2004;8(10):iii, 1–89.
2. O'Neill E, Hammond N, Miller FH. MR imaging of the pancreas. *Radiol Clin North Am* 2014;52(4):757–777.
3. Prabhakar PD, Prabhakar AM, Prabhakar HB, Sahani D. Magnetic resonance cholan-

- giopancreatography of benign disorders of the biliary system. *Magn Reson Imaging Clin N Am* 2010;18(3):497-514, xi.
- Vitellas KM, Keogan MT, Spritzer CE, Nelson RC. MR cholangiopancreatography of bile and pancreatic duct abnormalities with emphasis on the single-shot fast spin-echo technique. *RadioGraphics* 2000;20(4):939-957; quiz 1107-1108, 1112. [Published correction appears in *RadioGraphics* 2000;20(5):1494.]
  - Wong HP, Chiu YL, Shiu BH, Ho LC. Preoperative MRCP to detect choledocholithiasis in acute calculous cholecystitis. *J Hepatobiliary Pancreat Sci* 2012;19(4):458-464.
  - Ringe KI, Hartung D, von Falck C, Wacker F, Raatschen HJ. 3D-MRCP for evaluation of intra- and extrahepatic bile ducts: comparison of different acquisition and reconstruction planes. *BMC Med Imaging* 2014;14:16.
  - Yoon LS, Catalano OA, Fritz S, Ferrone CR, Hahn PF, Sahani DV. Another dimension in magnetic resonance cholangiopancreatography: comparison of 2- and 3-dimensional magnetic resonance cholangiopancreatography for the evaluation of intraductal papillary mucinous neoplasm of the pancreas. *J Comput Assist Tomogr* 2009;33(3):363-368.
  - Arizono S, Isoda H, Maetani YS, et al. High-spatial-resolution three-dimensional MR cholangiography using a high-sampling-efficiency technique (SPACE) at 3T: comparison with the conventional constant flip angle sequence in healthy volunteers. *J Magn Reson Imaging* 2008;28(3):685-690.
  - Matsunaga K, Ogasawara G, Tsukano M, Iwadata Y, Inoue Y. Usefulness of the navigator-echo triggering technique for free-breathing three-dimensional magnetic resonance cholangiopancreatography. *Magn Reson Imaging* 2013;31(3):396-400.
  - Morita S, Ueno E, Suzuki K, et al. Navigator-triggered prospective acquisition correction (PACE) technique vs. conventional respiratory-triggered technique for free-breathing 3D MRCP: an initial prospective comparative study using healthy volunteers. *J Magn Reson Imaging* 2008;28(3):673-677.
  - Almehdar A, Chavhan GB. MR cholangiopancreatography at 3.0 T in children: diagnostic quality and ability in assessment of common paediatric pancreatobiliary pathology. *Br J Radiol* 2013;86(1025):20130036.
  - Mugler JP 3rd, Bao S, Mulkern RV, et al. Optimized single-slab three-dimensional spin-echo MR imaging of the brain. *Radiology* 2000;216(3):891-899.
  - Arizono S, Isoda H, Maetani YS, et al. High spatial resolution 3D MR cholangiography with high sampling efficiency technique (SPACE): comparison of 3T vs. 1.5T. *Eur J Radiol* 2010;73(1):114-118.
  - Block KT, Uecker M, Frahm J. Undersampled radial MRI with multiple coils. Iterative image reconstruction using a total variation constraint. *Magn Reson Med* 2007;57(6):1086-1098.
  - Chandarana H, Feng L, Block TK, et al. Free-breathing contrast-enhanced multiphase MRI of the liver using a combination of compressed sensing, parallel imaging, and golden-angle radial sampling. *Invest Radiol* 2013;48(1):10-16.
  - Feng L, Grimm R, Block KT, et al. Golden-angle radial sparse parallel MRI: combination of compressed sensing, parallel imaging, and golden-angle radial sampling for fast and flexible dynamic volumetric MRI. *Magn Reson Med* 2014;72(3):707-717.
  - Lustig M, Donoho D, Pauly JM. Sparse MRI: The application of compressed sensing for rapid MR imaging. *Magn Reson Med* 2007;58(6):1182-1195.
  - Otazo R, Kim D, Axel L, Sodickson DK. Combination of compressed sensing and parallel imaging for highly accelerated first-pass cardiac perfusion MRI. *Magn Reson Med* 2010;64(3):767-776.
  - Vasanawala SS, Alley MT, Hargreaves BA, Barth RA, Pauly JM, Lustig M. Improved pediatric MR imaging with compressed sensing. *Radiology* 2010;256(2):607-616.
  - Li G, Hennig J, Raithel E, et al. An L1-norm phase constraint for half-Fourier compressed sensing in 3D MR imaging. *MAGMA* 2015;28(5):459-472.
  - Akansu AN, Haddad RA. Multiresolution signal decomposition: transforms, subbands, and wavelets. Orlando, Fla: Academic Press, 1992.
  - Beck A, Teboulle M. Fast gradient-based algorithms for constrained total variation image denoising and deblurring problems. *IEEE Trans Image Proc* 2009;18(11):2419-2434.
  - Stalder AF, Schmidt M, Quick HH, et al. Highly undersampled contrast-enhanced MRA with iterative reconstruction: Integration in a clinical setting. *Magn Reson Med* 2015;74(6):1652-1660.
  - Landis JR, Koch GG. The measurement of observer agreement for categorical data. *Biometrics* 1977;33(1):159-174.
  - Smith DS, Li X, Abramson RG, Quarles CC, Yankeelov TE, Welch EB. Potential of compressed sensing in quantitative MR imaging of cancer. *Cancer Imaging* 2013;13(4):633-644.
  - Rosenkrantz AB, Geppert C, Grimm R, et al. Dynamic contrast-enhanced MRI of the prostate with high spatiotemporal resolution using compressed sensing, parallel imaging, and continuous golden-angle radial sampling: preliminary experience. *J Magn Reson Imaging* 2015;41(5):1365-1373.
  - Glockner JF, Saranathan M, Bayram E, Lee CU. Breath-held MR cholangiopancreatography (MRCP) using a 3D Dixon fat-water separated balanced steady state free precession sequence. *Magn Reson Imaging* 2013;31(8):1263-1270.
  - Lavdas E, Vlychou M, Arikidis N, et al. How reliable is MRCP with an SS-FSE sequence at 3.0 T: comparison between SS-FSE BH and 3D-FSE BH ASSET sequences. *Clin Imaging* 2013;37(4):697-703.